ACS APPLIED MATERIALS & INTERFACES

Research Article

www.acsami.org

Simultaneous Electrospinning and Electrospraying: A Straightforward Approach for Fabricating Hierarchically Structured Composite Membranes

Nicolas Lavielle,[†,‡,§] Anne Hébraud,[†] Guy Schlatter,[†] Linda Thöny-Meyer,[‡] René M. Rossi,[§] and Ana-Maria Popa*[,§]

[†]Institut de Chimie et Procédés pour l'Energie, l'Environnement et la Santé, ICPEES-UMR7515, Université de Strasbourg, CNRS, Institut Carnot MICA, Ecole Européenne de Chimie, Polymères et Matériaux, 25 rue Becquerel, 67087 Strasbourg, cedex 2, France

[‡]Empa, Swiss Federal Laboratories for Materials Science and Technology, Laboratory for Biomaterials, Lerchenfeldstrasse 5, CH-9014 St. Gallen, Switzerland

[§]Empa, Swiss Federal Laboratories for Materials Science and Technology, Laboratory for Protection and Physiology, Lerchenfeldstrasse 5, CH-9014 St. Gallen, Switzerland

Supporting Information

ABSTRACT: We present here for the first time a simple method for micropatterning nonwoven composite membranes. The approach is based on the simultaneous electrospraying of microparticles and electrospinning of nanofibers from different polymer solution feeds (polyethylene glycol and poly(D,L-lactide)) on a common support. The mechanism of self-organization between fibers and particles into hierarchical honeycomb-like structures, as well as the evolution of the later as a function of the thickness of the composite, is investigated. We demonstrate that aggregates of particles, leading to a nonuniform distribution of the electrostatic field near the collector, are necessary to form the self-organized composite. Furthermore, it is shown that the specific dimensions of the generated patterns can be controlled by tuning the flow rate of electrospraying. The obtained composite mat exhibits a multilevel porous structure, with pore sizes ranging from few up to several hundreds of micrometers. Finally, it is shown that the microparticles can be selectively leached, allowing the production of a monocomponent membrane and retaining the hierarchical organization of the nanofibers suitable for biomedical and filtration applications.

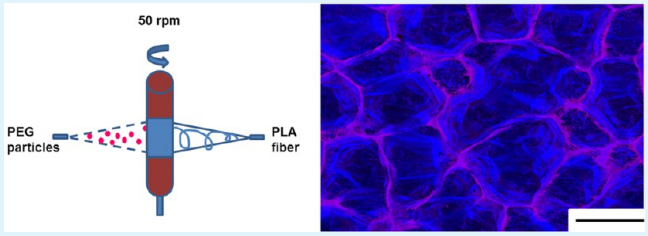

KEYWORDS: *self-organization, composite, nanofibers, microparticles, patterns, selective leaching*

INTRODUCTION

Electrospinning is widely used for the synthesis of nanofibrous nonwoven membranes.[1,2] The fabricated electrospun membranes have high porosities and high surface to volume ratio; they are thus suitable for many applications[3] such as sensing,[4] tissue engineering,[5] or drug delivery.[6] The electrospinning process usually leads to nonwoven mats by the random deposition of nanofibers. However, the control over the organization of nanofibers in electrospun membranes would provide a great benefit for various applications.[7] Indeed, precise geometric design of multicomponent electrospun membranes or 3D structures with defined porosity and pore sizes are necessary to mimic tissue structure and properties for tissue engineering applications[7,8] and to achieve spatially and temporally controlled release of different drugs for drug delivery applications.[9,10]

A number of methods have been developed to control the deposition of the nanofibers and prepare structured membranes. For example, aligned electrospun fibers have been obtained by electrospinning on a rotating collector.[11] More complex 2D or 3D structured membranes have also been prepared using electrostatic forces.[12−15] The principle of this approach is the modification of the electrostatic field near the collector, thus guiding the deposition of the charged nanofiber. In addition, structured membranes were also fabricated using diverse postelectrospinning structuring strategies: direct laser machining,[16] wetting of porous template,[17] or photopatterning of electrospun membranes.[18]

Another type of structured membranes can be obtained by the self-organization of electrospun nanofibers. They have been first presented by Deitzel et al.[19] for poly(ethylene oxide) and then observed for other polymers.[20−23] Such self-organized mats are very interesting for tissue engineering applications as they can form 3D centimeter-thick hierarchical foams with adequate pore sizes and mechanical properties.[23] It was shown that a bimodal distribution of the fiber diameter is a necessary

Received: July 5, 2013
Accepted: September 16, 2013
Published: October 7, 2013

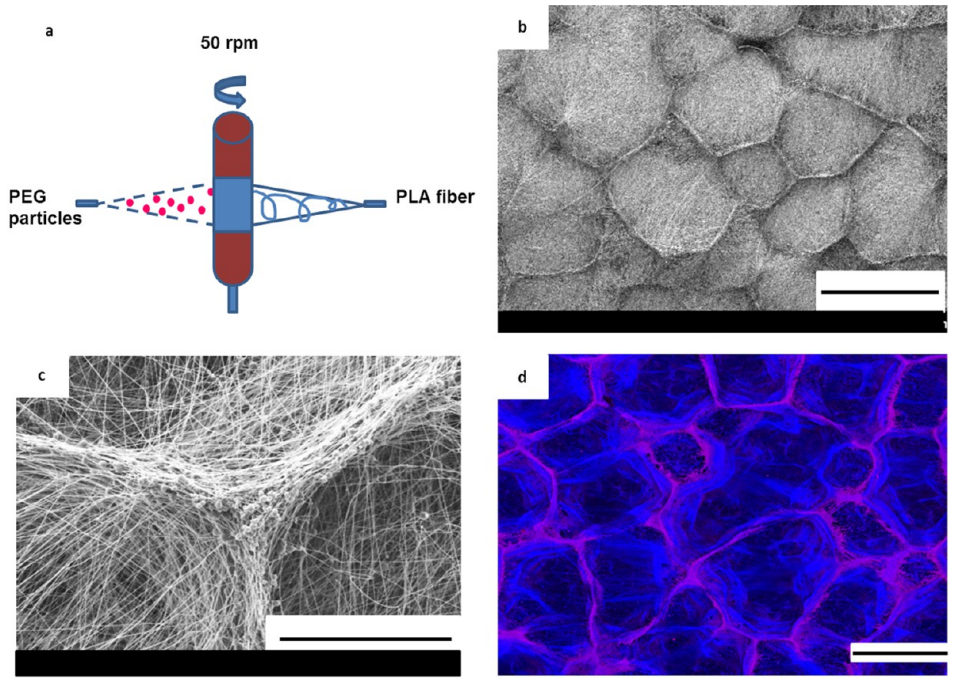

Figure 1. (a) Schematic illustration of the experimental setup. (b) SEM micrograph showing honeycomb-like patterns of the composite after 60 min of deposition (scale bar = 1 mm); (c) SEM micrograph of an elementary domain of a honeycomb-like pattern formed by the simultaneous electrospinning of PLA nanofibers and electrospraying of PEG microparticles after 60 min of deposition (scale bar = 50 μm); (d) Confocal fluorescent microscopy image of Lumogen Blue-loaded PLA nanofibers and Lumogen Pink-loaded PEG microparticles composite after 60 min of deposition (scale bar = 500 μm).

condition to induce the self-organization. Such irregular fibers, having thick and thin domains, locally impact the electrostatic field and guide the deposition of the fibers into honeycomb-like patterns.[23] However, a bimodal distribution of fiber diameters, leading to self-organization in the mat, is observed only in specific electrospinning conditions and is not easily transposable to every polymers. A solution to this problem could be the combination of electrospun monodisperse thin fibers with electrosprayed larger particles. This more versatile process results in composite membranes, in which fibers and particles of different polymers are combined, thus leading to added functionalities.

The fabrication of composite membranes has already been performed using dual or coelectrospinning,[24−26] which allows the combination of properties from different nanofibers within one membrane. Co-electrospinning has inspired the combination of electrospinning and electrospraying technologies to form a composite membrane made of electrospun fibers and electrosprayed particles. Electrospraying is very similar to electrospinning.[27] The main difference between these two processes is the presence and quantity of polymer chain entanglements in the polymer solution. Under identical electrospinning conditions, by simply decreasing the number of polymer chain entanglements in the solution, the morphology can be varied from regular nanofibers to beaded nanofibers and to particles.[28−30] Electrospinning and electrospraying can be performed simultaneously using a rotating mandrel and two capillaries through which the respective polymer solutions are fed; the yielded nano- and micro-objects are collected in a unique membrane. Hydrogels,[31] hydroxyapatite,[32] or even cells[33] have been simultaneously electrosprayed into electrospun scaffolds for tissue engineering and drug delivery applications. Finally, electrospraying is an efficient way for drug encapsulation into particles.[34] A comprehensive review on electrospraying of polymers with therapeutic molecules was recently published by Bock et al.[30]

In the present work, we develop a general method for the fabrication of structured electrospun composites. We demonstrate for the first time the self-organization of electrosprayed microparticles and regular thin electrospun nanofibers into growing honeycomb-like patterns. The obtained composites present a hierarchical porous structure with pore sizes ranging from a few micrometers up to hundreds of micrometers. The conditions allowing the formation of a structured or a random composite are discussed. The origin of the mechanism of the self-organization of fibers and particles, as well as the evolution of the generated patterns with the thickness of the composite are then investigated. Finally, we show the possibility of further varying the morphology of the composite membrane by the selective leaching of the particles.

EXPERIMENTAL SECTION

Materials. Poly(D,L-lactide) (PLA) of a molecular weight of 75 kg/mol and 15 kg/mol (values given by the supplier) were respectively supplied by Purac under the commercial names Purasorb PDL 0.6 and Purasorb PDL 0.2A. Acetic acid (purum ≥99.0%, H_2O ≈ 0.2%), formic acid (≈98%, H_2O ≈ 2%), and polyethylene glycol (PEG) of a molecular weight of 15 kg/mol were provided by Fluka (Sigma-Aldrich). The fluorescent dyes Lumogen F Pink 285 and Lumogen F Blue 650 were supplied by BASF. All products were used as received.

Electrospinning and Electrospraying Conditions. PLA nanofibers (75 kg/mol) were electrospun (ΔV = 24.5 kV, needle-collector distance =13.5 cm, pump flow rate = 0.3 mL/h, room temperature, 40% RH) from a solution of acetic acid/formic acid 50/50 (v/v) at the concentration of 22% (wt) 24 h after the preparation of the solution. PLA microparticles (15 kg/mol) were electrosprayed (V_{needle} = +28.5 kV, $V_{collector}$ = −1 kV, needle-collector distance =13.5 cm, pump flow rate = 0.3 mL/h, room temperature, 40% RH) from a solution of

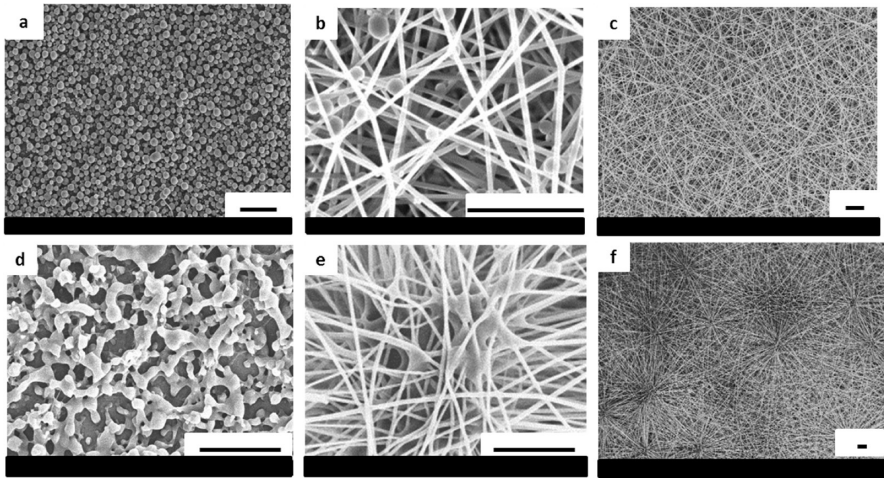

Figure 2. SEM micrographs of nonaggregated electrosprayed PLA particles (a); in the composite with PLA fibers at high (b) and low (c) magnifications; SEM micrographs of aggregated electrosprayed PLA particles (d); in the composite with PLA fibers at high (e) and low (f) magnifications. (scale bar = 5 μm).

acetic acid/formic acid 50/50 (v/v) at the concentration of 17% (wt) 24 h after the preparation of the solution for the fabrication of nonaggregated PLA particles and 48 h later for the fabrication of aggregated PLA particles. Indeed, after 48 h of solution preparation, the yielded particles were bigger (1.0 ± 0.2 μm compared to 540 ± 170 nm) and permitted aggregation.[35] PEG microparticles were electrosprayed (V_{needle} = +27 kV, $V_{collector}$ = −1 kV, needle-collector distance = 12 cm, pump flow rate = 0.08, 0.1, and 0.2 mL/h, 25 °C, 40% RH) from a solution of acetic acid/formic acid 10/90 (v/v) at the concentration of 55% (wt). The solvent mixture and the electrospinning−electrospraying conditions were optimized to obtain steady state formation of bead-free PLA nanofibers and spherical PLA and PEG microparticles. Fibers and particles were coelectrospun onto a vertical rotating drum as represented in Figure 1a. The rotation speed of the drum was 50 rpm and its diameter 4 cm. The rotation speed of the drum is low enough as not to contribute to fiber alignment. Moreover, in order to obtain a homogeneous mixture of the particles within the fibers, a dielectric tape was attached to the rotating collector to delimit the deposition area (5 cm) (Supporting Information (SI) Figure S3a and b). Indeed, without the dielectric tape and in the case of a larger deposition area of the particles than the one of the fibers, the charged electrosprayed particles will be deposited preferentially outside the dielectric nanofibrous mat, leading to an inhomogeneous or nonexisting composite. Charged electrosprayed particles are very sensitive to the electrostatic field and can be confined with a dielectric tape, as shown in SI Figure S3c. The components of the electrospinning setup have been described previously.[29] The fabricated composites were dried and stored in a dried atmosphere.

Characterization of the Composites. The morphology of the fibers, particles, and composites was characterized using a scanning electron microscope (SEM, Hitachi S-4800 at Vacc = 5 kV, Ie = 10 μA). Gold (5 nm) was sputtered on all membranes using a scanning electron microscope coating unit (E5100) from Polaron Equipment Limited. For each sample, the average nanofiber/microparticle diameter and standard deviation were calculated from the diameter measured from 12 nanofibers/microparticles in 3 randomly selected areas. A LSM 710−780 confocal fluorescent microscope from Zeiss was used to localize Lumogen Blue-loaded PLA fibers and Lumogen Pink-loaded PEG particles in the composite for Figure 1f. An optical microscope from Keyence was used to analyze the dimensions of the self-organized patterns, and ImageJ software was used for the analysis of images. The average linear pattern size (L) and the maximum pattern size (L_{max}) were calculated from three randomly selected areas per sample. Two lines were perpendiculary drawn on the images of the micropatterned membranes. The ratio between the length of the line and the number of crossed patterns is equal to L. Perpendicular lines were drawn to assess the orientation degree of the patterns. The maximum cross-path length of 20 patterns, randomly chosen, was measured. L_{max} is the average of these maximum lengths. Membranes thickness (h) was assessed using a profilometer (Dektak 150 from Veeco). To this end, composites were deposited when needed on Si wafers previously coated with 100 nm of aluminum and 10 nm of gold with an electron beam evaporator to ensure conductivity of the wafers. Otherwise, the composites were deposited on aluminum foils. Apparent density and porosity were determined gravimetrically using the following formulas, with m, the mass of the membrane and S, the membrane area:

$$\text{apparent density}\left(\frac{\text{g}}{\text{cm}^3}\right) = \frac{m}{hS}$$

$$\text{porosity} = \left(1 - \frac{\text{apparent density}}{\text{bulk density}}\right) \times 100$$

Transversal cut with Gillette blades at room temperature was performed to visualize cross sections of the composites (Figures 5 and 6).

RESULTS AND DISCUSSION

Self-Organization of Microparticles and Nanofibers. PEG particles and PLA fibers were electrosprayed and electrospun to generate a composite membrane. Figure 1a shows the setup used for the fabrication of the composite. PEG particles were electrosprayed on one side of the rotating collector, and PLA fibers were electrospun on the opposite side. This configuration is optimal for the coelectrospinning.[36] The process parameters were optimized in order to allow the steady state formation of bead-free PLA nanofibers and spherical PEG microparticles. PLA fibers (SI Figure S1a) and PEG particles (SI Figure S1b) had an average diameter of 200 ± 20 nm and 1.6 ± 0.4 μm, respectively. Both polymers were processed from an acetic acid and formic acid solvent mixture. This solvent system has been studied for the electrospinning of PCL[37] and as a tool to control the morphology of the yielded PCL electrospun fibers,[29] and it is successfully used for the production of PLA nanofibers and PEG microparticles.

In SI Figure S1a, when only fibers are deposited, a nonwoven electrospun mat with randomly placed PLA nanofibers can be observed. On the other hand, as shown in Figure 1b, the simultaneous electrospinning of PLA fibers and electrospraying of PEG particles leads to a uniquely structured composite

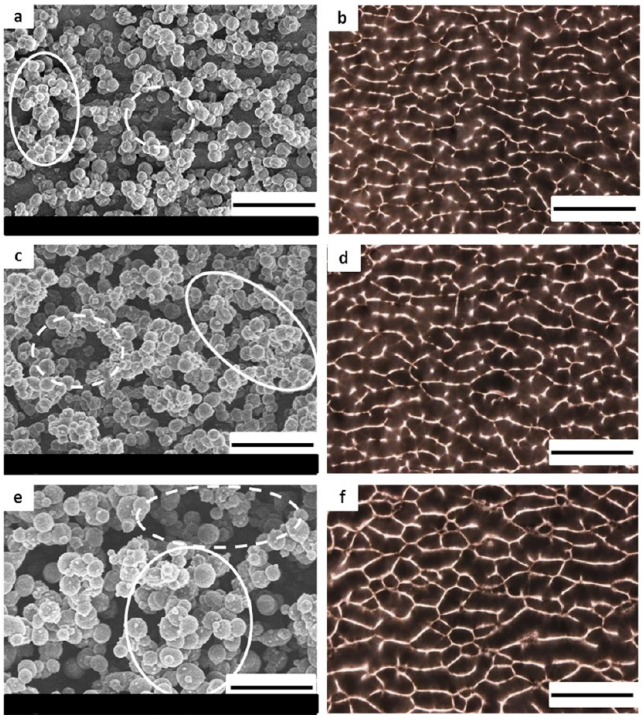

Figure 3. SEM micrographs of aggregated electrosprayed PEG particles at a flow rate of 0.08 mL/h (a), 0.1 mL/h (c) and 0.2 mL/h (e) after two minutes of deposition. Dashed and plain circles are showing empty and aggregated domains, respectively (scale bar = 10 μm). Optical microscopy images of the corresponding self-organized composites with PLA nanofibers obtained by simultaneous electrospraying and electrospinning (b, d, f) after 15 min of deposition (scale bar = 1 mm).

membrane with a honeycomb-like pattern. Indeed, after 1 h of deposition, honeycomb-like patterns with polydisperse sizes are observed. Such structures with honeycomb-like patterns have already been observed in simple electrospinning.[20−22] Ahirwal et al.[23] have shown that a bimodal distribution of fiber diameter was necessary to form these honeycomb-like patterns. The electrospinning of a fiber having thick and thin domains leads to the formation of a heterogeneous, rough surface that is nonuniformly charged. Indeed, thick domains, in contact with the collector, are areas where the electric charges can efficiently dissipate, while between these domains suspended thin fibers remain charged. These heterogeneities modulate the electrostatic field near the collector and act as a template for the formation of honeycomb-like patterns.[23] In our case, the electrosprayed PEG particles play the role of the thick domains whereas the regular PLA fibers play the role of the thin domains. As such, the respective morphologies of the thick or micrometer size domains and the thin or submicrometer size domains can be independently controlled. Figure 1c shows an elementary domain of the honeycomb-like pattern. We notice that the particles are mainly located in the walls forming the borders of the patterns. In order to confirm this observation, a membrane with stained fibers and particles was fabricated. Lumogen blue fluorescent dye was added to the PLA solution feed and Lumogen pink dye to the PEG solution feed. Confocal fluorescence microscopy (Figure 1d) confirmed that particles and fibers are preferentially deposited in the walls of the honeycomb-like pattern whereas, between the walls, only stretched nanofibers are present. This result is in agreement with the observations made with the self-organization of irregular fibers.[23] Indeed, particles are independent entities, whereas an electrospun fiber can be viewed as a continuous cylinder. To cross the repulsive area formed by the charged fibers inside a pattern from one wall to another, the next particle will just deposit directly on the next wall, whereas the fiber has the possibility of crossing the pattern to reach the next wall or to align along the wall as a consequence of the confinement effect.[12,14]

The patterns are formed by the self-organization of the fibers and the particles. In the first moments of the deposition, particles and fibers form a nonuniform, rough surface. This heterogeneous surface is used as a template for the deposition of the following particles and fibers. In Figure S1b, (Supporting Information) we observe that when only electrospraying is carried out the particles are not deposited homogeneously over the surface but are aggregated and form a heterogeneous surface with randomly distributed domains of high and low densities of particles. Again, this observation can be compared with the first moments of the deposition of irregular fibers where some locations showed aggregated thick fiber domains and others thin fiber domains.[23] As discussed before, the nonuniform surface would be the basis for the self-organization of the composite. We thus hypothesize that aggregated particles (or larger particles) are necessary to form the patterns generating a nonuniform electrostatic field. To confirm this hypothesis, we investigated the influence of the aggregation of the microparticles on the self-organization process. Dielectric particles of the same electric charge can be attracted to one another depending on the range of particle size and charge ratios.[35,38,39] As the particle size increases, the attractive force becomes stronger.[35] Unfortunately, we were not able to produce nonaggregated PEG particles because we could not decrease their sizes sufficiently with the used solvent system. Thus, for this demonstration only, PLA was used to produce the particles. Indeed, we found similar conditions (i.e., in the same solvent system) allowing electrospraying of nonaggregated PLA particles (Figure 2a) and aggregated PLA particles (Figure 2d). Aggregated and nonaggregated particles of PLA were fabricated because their individual size could be tuned from few hundred of nanometers in diameter (540 ± 170 nm) up to micrometer size (1.0 ± 0.2 μm). When nonaggregated particles were electrosprayed in combination with PLA nanofibers, a uniform distribution of them within the fiber mesh was observed (Figure 2b) leading to a composite membrane with randomly deposited particles and fibers (Figure 2c). On the contrary, for aggregated electrosprayed particles (Figure 2d), their combination with electrospun nanofibers resulted in a heterogeneous distribution of the particles within the membrane (Figure 2e). As a consequence, a nonuniform charge distribution was formed over the surface. The deposition of the incoming fibers was then guided by these heterogeneities in the electric field and micrometric patterns were generated (Figure 2f).

It is thus clear that the aggregation degree plays a major role in the formation of patterned composites. We can make the assumption that by varying the size of the aggregated domains one can fine-tune the self-organization of the incoming fibers. To verify this hypothesis, a PEG solution was electrosprayed at different flow rates. This led to the formation of particles of different sizes and quantities. Parts a, c, and e of Figure 3 show that aggregated PEG particles with average diameters D = 1.3 ± 0.2 μm, 1.6 ± 0.4 μm, and 2.4 ± 0.5 μm can be obtained with

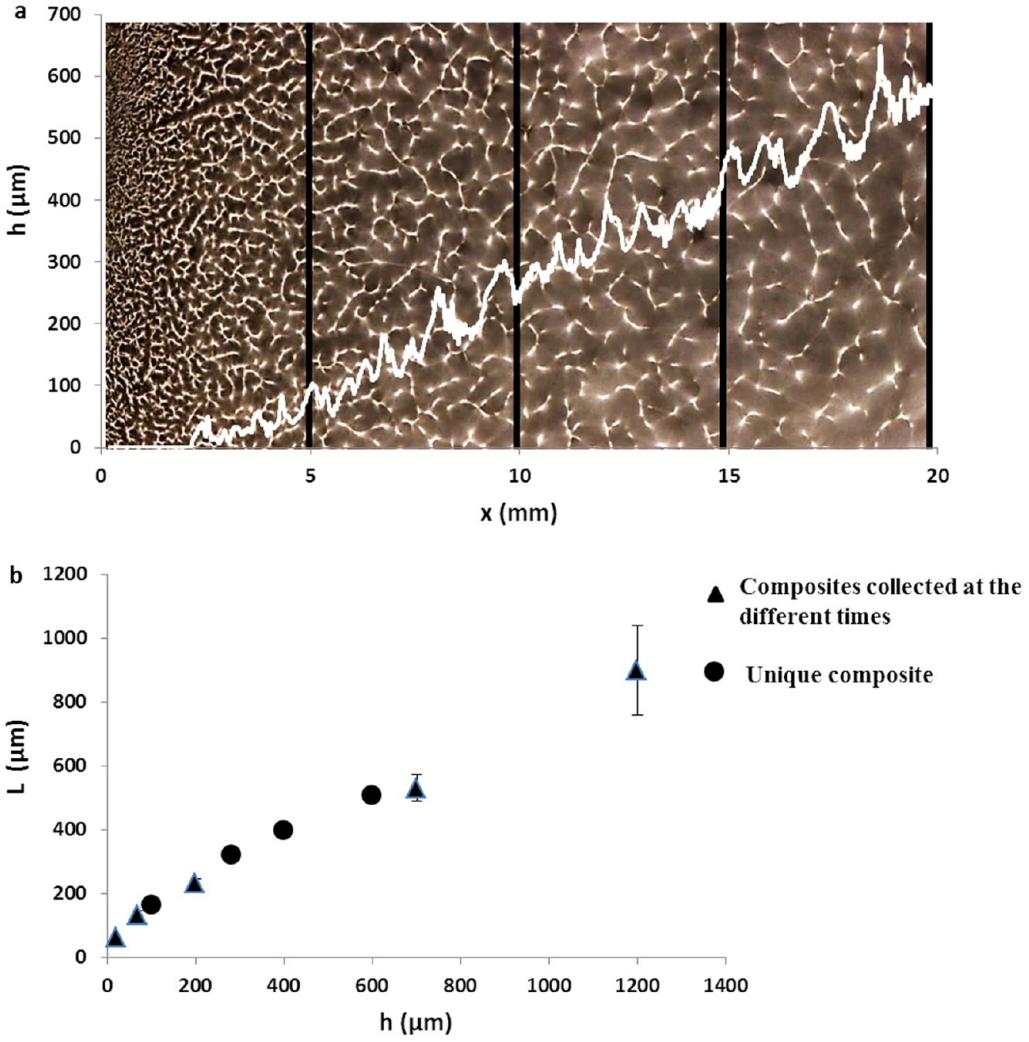

Figure 4. (a) Evolution of the membrane thickness (h) as a function of the distance (x) and optical microscopy image of the corresponding membrane. L was determined for x equal to 5, 10, 15, and 20 mm represented by the black vertical lanes. (b) Evolution of the average linear pattern size (L) with standard deviation as a function of the membrane thickness (h).

flow rates q of 0.08 mL/h (PEG 0.08), 0.1 mL/h (PEG 0.1), and 0.2 mL/h (PEG 0.2), respectively. All particles were found to be aggregated on the surface of the collector after simple electrospraying. Because the deposition area was the same for the three kinds of particles and the PEG solution was the same for all experiments, one can assume that the number of particles produced during a given time is proportional to q/D^3. Thus, the lowest flow rate leads to the production of the highest number of the smallest particles. More precisely, PEG 0.08 yielded 1.5 times more particles than PEG 0.1, which yielded 1.7 times more particles than PEG 0.2. The variation of the flow rate is thus a straightforward manner to modulate the number and the size of the particles but unfortunately not independently. As a consequence, the size of the aggregated particles domains (plain white circles in Figure 3) and the empty domains (dashed white circles in Figure 3) can also be tuned. A higher number of smaller particles lead to smaller particle aggregates and to smaller neighboring empty domains. Looking at the corresponding self-organized composites made of the particles and the nanofibers (Figure 3 b, d, and f), we can observe the influence of the electrospraying flow rate on the pattern size for the same production time (15 min). The differences in the pattern sizes can be quantified. We can define L, the average characteristic pattern size, defined as $L = L_0/N$, with N, the number of patterns crossed by a line of length L_0. We also define p, a polydispersity index of the size distribution of the patterns with $p = p'/L_{max}$, where L_{max} is the average of the maximum length of the patterns and p' its standard deviation. We found (L = 290 μm; p = 0.4) when PEG 0.08 was used, (L = 345 μm; p = 0.4) with PEG 0.1, and (L = 410 μm; p = 0.5) with PEG 0.2.

In conclusion, by increasing the particle flow rate, one can obtain larger aggregate sizes and thus increase the characteristic size L of the honeycomb-like patterns. Consequently, the independent production of particles and nanofibers allows the control over the size of the honeycomb-like pattern by varying a simple experimental parameter. This is not possible in the case of the self-organization induced by bimodal nanofibers.

However, one can notice in Figure 3 that the size of the aggregated and related empty domains, in the range of 10 μm, is much smaller than the size L of the patterns, in the range of few hundreds of micrometers, obtained after 15 min of deposition. A closer observation of the samples shows an increasing pattern size from the edges to the center of the membrane. Indeed, the deposition is not exactly uniform as more fibers and particles are deposited in the center of the

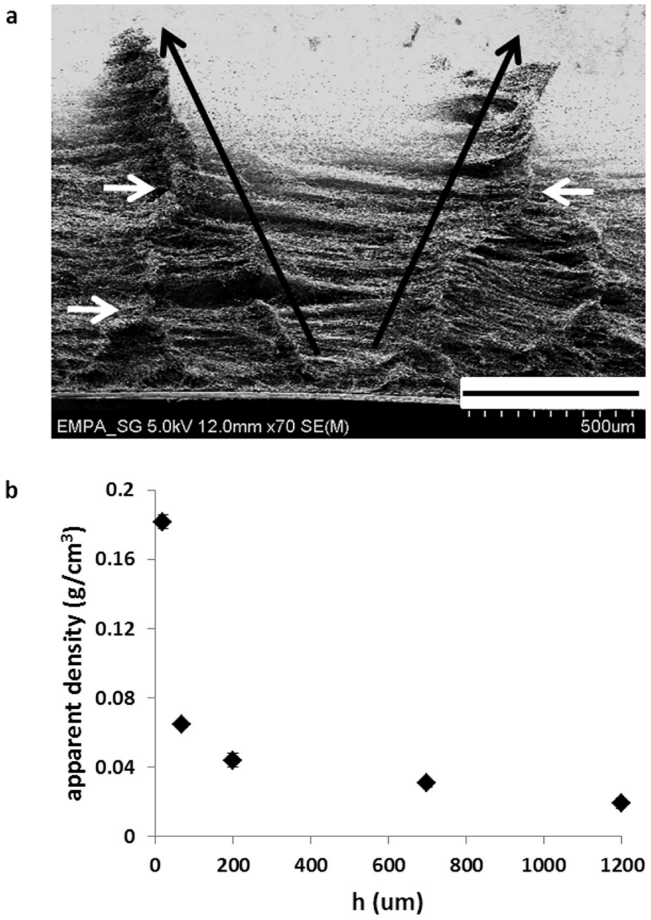

Figure 5. (a) SEM micrograph of a cross-section of the self-organized (scale bar = 500 μm) composite made of PLA nanofibers and PEG 0.1 microparticles after 1 h of deposition, showing in the center a growing pattern (black arrows) and on the two sides patterns merging into a unique one (white arrows). (b) Evolution of the apparent density of the composite membrane as a function of its thickness (h).

collector than on the edges. Moreover, the pattern sizes appear to increase with deposition times until becoming visible on a macroscopic scale.

Evolution of Pattern Size with the Thickness of the Sample. In order to understand how the self-organized pattern can grow from a few micrometers to several hundred of micrometers and characterize the structure of the membranes, the evolution of pattern size with thickness of the membrane was investigated. For this purpose, electrosprayed PEG 0.1 particles and electrospun PLA fibers were deposited simultaneously on conductive wafers clamped on the rotating collector and observed at the deposition times of 5, 10, 20, 40, and 60 min.

For each sample, the thickness profile of the composite was analyzed by profilometry. Figure 4a shows the typical thickness profile of the membrane after 40 min of deposition from the edge of the wafer (x = 0) toward its center (x = 20 mm). The growing of the patterns as a function of the thickness can be clearly observed on the optical microscopy image of the sample superimposed with the profile. The average linear pattern size (L) of the membrane was measured for (x = 5, 10, 15, 20) mm (Figure 4a, black vertical lines) and plotted as a function of h, the membrane thickness (Figure 4b). The additional points on the graph of Figure 4b correspond to measurements taken from the center of samples obtained after the different deposition times (optical microscopy images in Figure S2, Supporting Information). All measurements are in good agreement with each other and fit to the same curve. An increase of the size of the patterns with the thickness has also been observed and explained by Ahirwal et al.[23] for the self-organization of bimodal fibers. It originates from the broad size distribution of the first generated patterns. Electrostatics numerical simulation on such a surface show a higher vertical component of the electrostatic field over the walls of larger patterns, leading to the preferential deposition on the bigger patterns and the progressive disappearance of the smaller ones. In our case also, a size polydispersity of aggregates and patterns can be observed (Figure 3c and d), and thus, the evolution of the patterns can be explained by a similar mechanism. The fabricated composites thus exhibit a hierarchical structure with patterns gradually growing with the thickness of the composite.

Figure 5 shows a SEM micrograph of the cross-section of a 1 mm-thick composite membrane made of electrosprayed PEG 0.1 particles and PLA nanofibers after 1 h of deposition. Additionally to the pores formed by the interfiber distance, we can observe larger pores formed between the walls of the patterns and directly related to the pattern size L.[23] The size of the large pores increases with the thickness of the sample, as the size (L) of the formed patterns is growing. In Figure 5a, the main central pattern (black arrows) has pore sizes ranging from few micrometers at the bottom part up to around one millimeter at the top part of the membrane. Furthermore, on both sides of the image two walls merging into a unique one (white arrows) can be seen, showing the pattern growth as discussed previously. The self-organization of particles and fibers into growing honeycomb-like patterns results in a hierarchical porosity and a global increase of the pore size within the thickness of the membrane. Figure 5b presents the evolution of the apparent density of the membrane as a function of its thickness. We can observe that the apparent density decreases with h and the value is divided by ten over the thickness of the membrane. The corresponding porosity varies from 85 to 98% over the thickness.

Application to the Fabrication of Hierarchical Porous Membranes by the Selective Leaching of the Electrosprayed Particles. The composite presented here has the additional advantage of being formed by two distinct materials. This allows the design of composites with added functionality by choosing appropriate materials for the intended final application. It is moreover possible to remove selectively one of the two materials by selective leaching. Selective leaching is a strategy that has already been used with coelectrospinning. Selective removal of sacrificial fibers was used to improve cell infiltration in electrospun scaffolds[40] or particle-loaded sacrificial fibers were used to deposit the particles into an electrospun mat.[41] In our case, selective leaching of the particles would allow to have an electrospun membrane formed of regular self-organized nanofibers. To this end, the composite membrane made of PEG 0.1 microparticles and PLA nanofibers was washed in a 500 mL bath of deionized water during 10 min in order to remove the water-soluble PEG and obtain a pure PLA nonwoven. Figure 6 presents SEM images of the membrane before (a, c, and e) and after washing (b, d, and f). Comparing parts a and b in Figure 6, we can notice that the microstructure formed by the patterns is maintained even after the removal of the PEG particles. A closer look to the walls of the patterns, where the particles are located (Figure 6c)

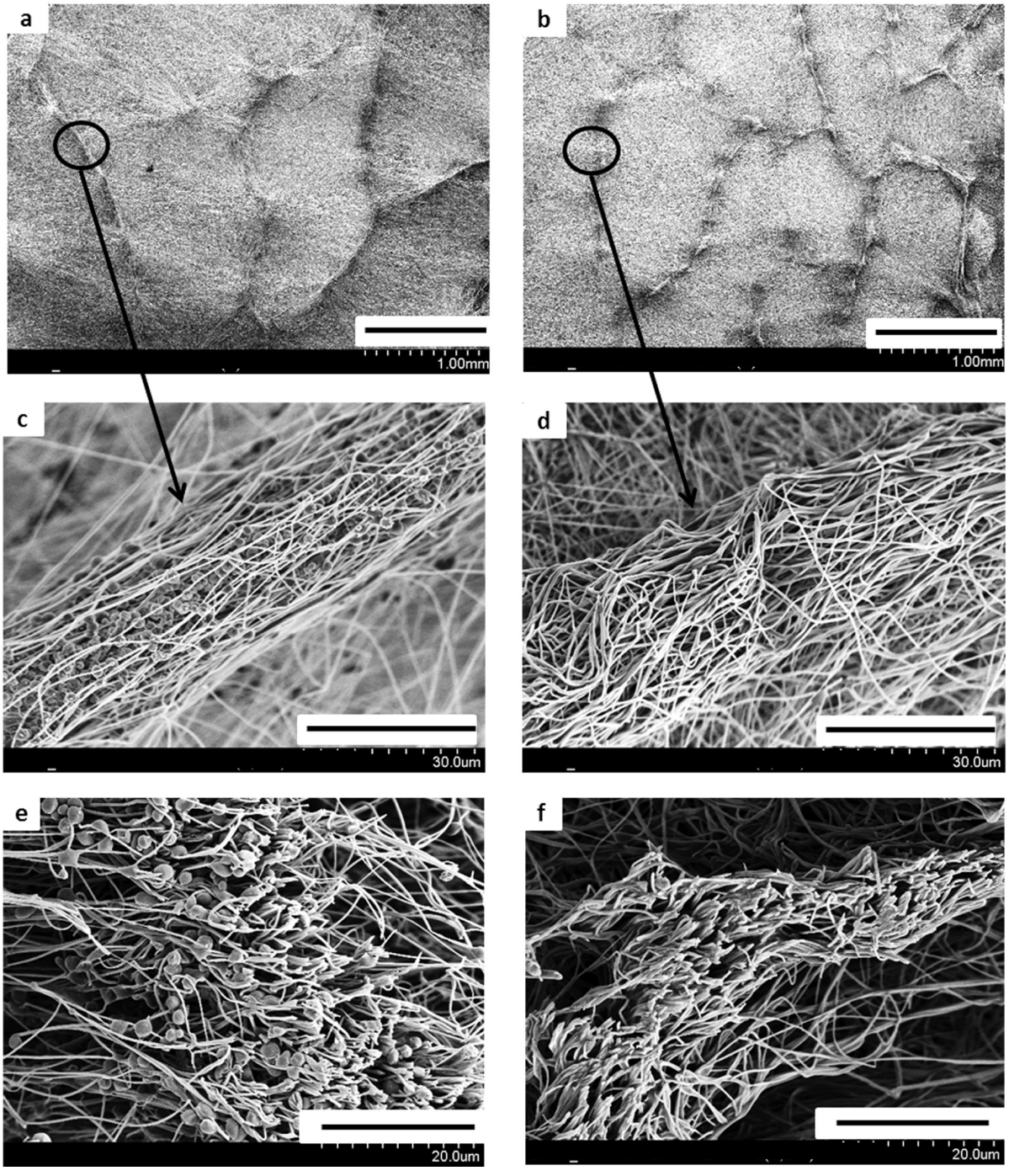

Figure 6. SEM micrographs of the self-organized composite made of PLA nanofibers and PEG0.1 microparticles before (a, c, e) and after (b, d, f) particles leaching. (e, f) Cross-section images of the composite.

confirms the disappearance of the PEG particles (Figure 6d). The same observation can be made on the basis of the cross-sectional images acquired before and after washing (Figure 6e and f respectively). Since the particles and fibers can be generated independently from materials with different properties, it is easily possible to generate a monocomponent microstructured membrane from a multicomponent one.

The processing approach described in this work allows the formation of three-dimensional scaffolds, which are of paramount importance for tissue engineering.[23] In particular, the technology presented here is not limited to certain polymer systems, and it allows also the combination of inorganic particles with polymeric matrices. The method also allows the fabrication of scaffolds with large pores having diameters in the tens of micrometers range, sizes which are comparable to different cell types. As a particular application we can cite bone tissue engineering, where an open, multilevel structured support is essential for ensuring cell infiltration and proliferation.[42−44] Such hierarchically structured membranes are also very interesting for biological fluids filtration, as they allow the size selective separation of cells, macro- and small molecular components respectively.[45]

CONCLUSIONS

Electrosprayed microparticles and electrospun nanofibers can self-organize to form a unique honeycomb-like composite. The driving force of the organization process is the local variation of the electric field when aggregated particles are used. The specific pattern dimensions can be controlled by varying a simple experimental parameter, the electrospraying flow rate. Moreover, millimeter-thick samples can be easily prepared with hierarchical porosity and increasing pore sizes that are preserved after selective removal of the particles. This technique is suitable for any other material, as long as aggregated particles are obtained. The combination of electrospinning and electrospraying technologies thus enables the fabrication of new types of structured composite membranes, interesting for a wide range of biomedical applications.

ASSOCIATED CONTENT

Supporting Information

Additional information including composite fabrication and characterization. This material is available free of charge via the Internet at http://pubs.acs.org.

AUTHOR INFORMATION

Corresponding Author

*E-mail: ana-maria.popa@empa.ch.

Notes

The authors declare no competing financial interest.

REFERENCES

(1) Reneker, D. H.; Yarin, A. L. *Polymer* **2008**, *49*, 2387−2425.
(2) Reneker, D. H.; Chun, I. *Nanotechnology* **1996**, *7*, 216−223.
(3) Greiner, A.; Wendorff, J. H. *Angew. Chem., Int. Ed.* **2007**, *46*, 5670−5703.
(4) Popa, A. M.; Eckert, R.; Crespy, D.; Rupper, P.; Rossi, R. M. *J. Mater. Chem.* **2011**, *21*, 17392−17395.
(5) Guex, A. G.; Kocher, F. M.; Fortunato, G.; Korner, E.; Hegemann, D.; Carrel, T. P.; Tevaearai, H. T.; Giraud, M. N. *Acta Biomater.* **2012**, *8*, 1481−1489.
(6) Sill, T. J.; von Recum, H. A. *Biomaterials* **2008**, *29*, 1989−2006.
(7) Szentivanyi, A.; Chakradeo, T.; Zernetsch, H.; Glasmacher, B. *Adv. Drug Delivery Rev.* **2011**, *63*, 209−220.
(8) Bottino, M. C.; Thomas, V.; Janowski, G. M. *Acta Biomater.* **2011**, *7*, 216−224.
(9) Bonani, W.; Motta, A.; Migliaresi, C.; Tan, W. *Langmuir* **2012**, *28*, 13675−13687.
(10) Okuda, T.; Tominaga, K.; Kidoaki, S. *J. Controlled Release* **2010**, *143*, 258−264.
(11) Katta, P.; Alessandro, M.; Ramsier, R. D.; Chase, G. G. *Nano Lett.* **2004**, *4*, 2215−2218.
(12) Li, D.; Ouyang, G.; McCann, J. T.; Xia, Y. N. *Nano Lett.* **2005**, *5*, 913−916.
(13) Murugan, R.; Ramakrishna, S. *Tissue Eng.* **2007**, *13*, 1845−1866.
(14) Lavielle, N.; Hébraud, A.; Mendoza-Palomares, C.; Ferrand, A.; Benkirane-Jessel, N.; Schlatter, G. *Macromol. Mater. Eng.* **2012**, *297*, 958−968.
(15) Zhang, D. M.; Chang, J. *Nano Lett.* **2008**, *8*, 3283−3287.
(16) Huaqiong, Li, Y. S. W.; Wen, F.; Ng, K. W.; Ng, G. K. L.; Venkatraman, S. S.; Boey, F. Y. C.; Tan, L. P. *Macromol. Biosci.* **2013**, *13*, 299−310.
(17) Chen, J. T.; Chen, W. L.; Fan, P. W. *ACS Macro Lett.* **2012**, *1*, 41−46.
(18) Sundararaghavan, H. G.; Metter, R. B.; Burdick, J. A. *Macromol. Biosci.* **2010**, *10*, 265−270.
(19) Deitzel, J. M.; Kleinmeyer, J.; Harris, D.; Tan, N. C. B. *Polymer* **2001**, *42*, 261−272.
(20) Thandavamoorthy, S.; Gopinath, N.; Ramkumar, S. S. *J. Appl. Polym. Sci.* **2006**, *101*, 3121−3124.
(21) Ye, X. Y.; Huang, X. J.; Xu, Z. K. *Chin. J. Polym. Sci.* **2012**, *30*, 130−137.
(22) Yan, G. D.; Yu, J.; Qiu, Y. J.; Yi, X. H.; Lu, J.; Zhou, X. S.; Bai, X. D. *Langmuir* **2011**, *27*, 4285−4289.
(23) Ahirwal, D.; Hébraud, A.; Kádár, R.; Wilhelm, M.; Schlatter, G. *Soft Matter* **2013**, *9*, 3164−3172.
(24) Ladd, M. R.; Lee, S. J.; Stitzel, J. D.; Atala, A.; Yoo, J. J. *Biomaterials* **2011**, *32*, 1549−1559.
(25) Hong, Y.; Fujimoto, K.; Hashizume, R.; Guan, J. J.; Stankus, J. J.; Tobita, K.; Wagner, W. R. *Biomacromolecules* **2008**, *9*, 1200−1207.
(26) Bonani, W.; Maniglio, D.; Motta, A.; Tan, W.; Migliaresi, C. *J. Biomed. Mater. Res., Part B* **2011**, *96B*, 276−286.
(27) Jaworek, A. *J. Mater. Sci.* **2007**, *42*, 266−297.
(28) Morota, K.; Matsumoto, H.; Mizukoshi, T.; Konosu, Y.; Minagawa, M.; Tanioka, A.; Yamagata, Y.; Inoue, K. *J. Colloid Interface Sci.* **2004**, *279*, 484−492.
(29) Lavielle, N.; Popa, A. M.; de Geus, M.; Hébraud, A.; Schlatter, G.; Thöny-Meyer, L.; Rossi, R. M. *Eur. Polym. J.* **2013**, *49*, 1331−1336.
(30) Bock, N.; Dargaville, T. R.; Woodruff, M. A. *Prog. Polym. Sci.* **2012**, *37*, 1510−1551.
(31) Ekaputra, A. K.; Prestwich, G. D.; Cool, S. M.; Hutmacher, D. W. *Biomacromolecules* **2008**, *9*, 2097−2103.
(32) Gupta, D.; Venugopal, J.; Mitra, S.; Dev, V. R. G.; Ramakrishna, S. *Biomaterials* **2009**, *30*, 2085−2094.
(33) Stankus, J. J.; Soletti, L.; Fujimoto, K.; Hong, Y.; Vorp, D. A.; Wagner, W. R. *Biomaterials* **2007**, *28*, 2738−2746.
(34) Valo, H.; Peltonen, L.; Vehvilainen, S.; Karjalainen, M.; Kostiainen, R.; Laaksonen, T.; Hirvonen, J. *Small* **2009**, *5*, 1791−1798.
(35) Chu, X. L.; Wasan, D. T. *J. Colloid Interface Sci.* **1996**, *184*, 268−278.
(36) Stankus, J. J.; Guan, J. J.; Fujimoto, K.; Wagner, W. R. *Biomaterials* **2006**, *27*, 735−744.
(37) Van der Schueren, L.; De Schoenmaker, B.; Kalaoglu, O. I.; De Clerck, K. *Eur. Polym. J.* **2011**, *47*, 1256−1263.
(38) Bichoutskaia, E.; Boatwright, A. L.; Khachatourian, A.; Stace, A. J. *J. Chem. Phys.* **2010**, *133*, 024105.
(39) Stace, A. J.; Boatwright, A. L.; Khachatourian, A.; Bichoutskaia, E. *J. Colloid Interface Sci.* **2011**, *354*, 417−420.
(40) Baker, B. M.; Gee, A. O.; Metter, R. B.; Nathan, A. S.; Marklein, R. A.; Burdick, J. A.; Mauck, R. L. *Biomaterials* **2008**, *29*, 2348−2358.
(41) Ionescu, L. C.; Lee, G. C.; Sennett, B. J.; Burdick, J. A.; Mauck, R. L. *Biomaterials* **2010**, *31*, 4113−4120.
(42) Eap, S.; Ferrand, A.; Palomares, C. M.; Hébraud, A.; Stoltz, J. F.; Mainard, D.; Schlatter, G.; Benkirane-Jessel, N. *Bio-Med. Mater. Eng.* **2012**, *22*, 137−141.
(43) Vitale-Brovarone, C.; Baino, F.; Verne, E. *J. Biomater. Appl.* **2010**, *24*, 693−712.
(44) Karageorgiou, V.; Kaplan, D. *Biomaterials* **2005**, *26*, 5474−5491.
(45) Bruil, A.; Feijen, J.; Wenzel-Rejda, T. (NPBI Nederlands Produktielaboratorium voor Bloedtransfusieapparatuur en Infusievloeistoffen B.V.). Patent No. EP0406485 A1, January 9, 1991.